Inflammatory cytokines down-regulate the barrier-protective prostasin-matriptase proteolytic cascade early in experimental colitis

Received for publication, December 6, 2016, and in revised form, May 2, 2017 Published, Papers in Press, May 10, 2017, DOI 10.1074/jbc.M116.771469

Marguerite S. Buzza[‡], Tierra A. Johnson[‡], Gregory D. Conway[‡], Erik W. Martin[‡], Subhradip Mukhopadhyay[‡], Terez Shea-Donohue[§], and Toni M. Antalis[‡1]

From the [‡]Center for Vascular and Inflammatory Diseases and Department of Physiology and the [§]Department of Radiation Oncology, University of Maryland School of Medicine, Baltimore, Maryland 21201

Edited by Luke O'Neill

Compromised gastrointestinal barrier function is strongly associated with the progressive and destructive pathologies of the two main forms of irritable bowel disease (IBD), ulcerative colitis (UC), and Crohn's disease (CD). Matriptase is a membrane-anchored serine protease encoded by suppression of tumorigenicity-14 (*ST14*) gene, which is critical for epithelial barrier development and homeostasis. Matriptase barrier-protective activity is linked with the glycosylphosphatidylinositol (GPI)-anchored serine protease prostasin, which is a co-factor for matriptase zymogen activation. Here we show that mRNA and protein expression of both matriptase and prostasin are rapidly down-regulated in the initiating inflammatory phases of dextran sulfate sodium (DSS)-induced experimental colitis in mice, and, significantly, the loss of these proteases precedes the appearance of clinical symptoms, suggesting their loss may contribute to disease susceptibility. We used heterozygous *St14* hypomorphic mice expressing a promoter-linked β-gal reporter to show that inflammatory colitis suppresses the activity of the *St14* gene promoter. Studies in colonic T84 cell monolayers revealed that barrier disruption by the colitis-associated Th2-type cytokines, IL-4 and IL-13, down-regulates matriptase as well as prostasin through phosphorylation of the transcriptional regulator STAT6 and that inhibition of STAT6 with suberoylanilide hydroxamic acid (SAHA) restores protease expression and reverses cytokine-induced barrier dysfunction. Both matriptase and prostasin are significantly down-regulated in colonic tissues from human subjects with active ulcerative colitis or Crohn's disease, implicating the loss of this barrier-protective protease pathway in the pathogenesis of irritable bowel disease.

Inflammatory bowel diseases (IBD)[2] ulcerative colitis (UC) and Crohn's disease (CD) are associated with inflammation of the gastrointestinal tract that arises from a dysregulated immune response to both bacteria and bacterial products in genetically predisposed individuals (reviewed in Refs. 1 and 2). The pathogenesis of IBD is still unclear, but increasing evidence shows that compromised intestinal epithelial barrier function is strongly associated with IBD susceptibility and progression (3–6). Antigen-induced inflammatory cytokines in the intestinal submucosa are believed to play a central role in the pathogenesis of human IBD (7–9), perpetuating the increased intestinal permeability and causing cyclical bouts of painful inflammation. In general, mucosal inflammation in CD is associated with increased expression of T helper (Th) 1 and Th17 cytokines (*e.g.* IFNγ, IL-17A), whereas UC is associated with Th2 cytokines such as IL-4, IL-10, and IL-13. Both disease states converge in the production of TNFα, which activates multiple pro-inflammatory pathways and contributes to epithelial barrier disruption (reviewed in Ref. 10).

Th1 and Th2 inflammatory cytokines present in human IBD tissue increase intestinal permeability by inducing the internalization and loss of barrier-protective junctional proteins from the cell surface (*e.g.* E-cadherin, occludin, zonula occludens-1 (ZO-1)) (11, 12), leading to increased paracellular permeability to macromolecules (11, 12), and also by increasing the expression and junctional localization of permeability-associated tight junction proteins such as claudin-2, which forms paracellular pores mediating cation and water flux (13, 14). Elevated claudin-2 expression is found in inflamed villus epithelium of patients with active IBD, correlating with disease severity (15, 16). Studies using human colonic epithelial monolayers show that claudin-2 mRNA and protein are specifically induced by Th2 cytokines IL-13 and IL-4, but not Th1 cytokines TNFα or IFNγ (8, 13, 17).

IL-13 is considered a critical effector cytokine in UC (8, 18), where lymphocytes in the lamina propria produce substantially more IL-13 than healthy individuals and CD patients do (9, 19, 20). The functional importance of IL-13 is underscored by the finding that neutralization of IL-13 prevents oxazalone-induced colitis (8), a mouse model with similar features to human

This work was supported by U.S. Department of Defense Grant PR110378 and National Institutes of Health Grants R01 DK081376 and R01 HL118390 (T. M. A.) and R01 DK83418 (T. S. D.). The authors declare that they have no conflicts of interest with the contents of this article.The content is solely the responsibility of the authors and does not necessarily represent the official views of the National Institutes of Health.

This article contains supplemental Fig. S1.

[1] To whom correspondence should be addressed: 800 West Baltimore Street, Baltimore, MD 21201. Tel.: 410-706-8222; Fax: 410-706-8121; E-mail: tantalis@som.umaryland.edu.

[2] The abbreviations used are: IBD, inflammatory bowel disease; CD, Crohn's disease; DSS, dextran sodium sulfate; GPI, glycosylphosphatidylinositol; GT, gene trap; IFN, interferon; IL, interleukin; OCT, optimal cutting temperature compound; SAHA, suberoylanilide hydroxamic acid; STAT, signal transducer and activation of transcription; TEER, transepithelial electrical resistance; Th, T helper; TJ, tight junction; TNF, tumor necrosis factor; UC, ulcerative colitis.

UC. However, antibody-based IL-13 blockade for the treatment of UC has been ineffective in two independent clinical trials (21), suggesting a more complex cytokine milieu in humans. IL-4 expression is also elevated in rectal mucosa of patients with active UC (16), and deficiency or inhibition of IL-4 results in reduced disease severity in murine models of ulcerative colitis (22, 23). The potential use of a dual antagonist of IL-4 and IL-13 is currently being explored and has also shown promising results in mice (24).

Multiple studies using genetic ablation approaches in mice have demonstrated an essential role for the membrane-anchored serine protease matriptase (also known as MT-SP1, TADG-15, epithin, and SNC19) (25) in the formation and maintenance of epithelial barriers in the intestine and skin (26–30). In prior studies, we investigated the role of matriptase in intestinal barrier function and protection against DSS-induced inflammatory colitis using *St14* hypomorphic mice, which express 1–5% of normal matriptase levels and demonstrate both increased paracellular macromolecular permeability and paracellular ion flux that is associated with increased claudin-2 expression (29, 30). Increased macromolecular permeability and increased claudin-2 are also associated with siRNA-mediated knockdown of matriptase in human intestinal epithelial Caco-2 monolayers, which fail to develop an epithelial barrier (29, 31). Matriptase is found localized to epithelial adherens junctions (29, 32), and indirectly mediates the post-translational turnover of claudin-2 (29). Although the precise mechanisms are still unclear, these studies demonstrate a critical role for matriptase in regulating intestinal epithelial barrier closure that protects against colitis.

The barrier-protective activities of matriptase in intestinal epithelium can be regulated by an upstream GPI-anchored serine protease, prostasin. Whereas matriptase has the capacity to auto-activate (33, 34), prostasin appears to function as a co-factor for matriptase zymogen activation (35, 36), an activity that may be independent of prostasin's proteolytic activity (32). Like matriptase, depletion of prostasin in Caco-2 intestinal epithelial monolayers inhibits barrier development, and the addition of recombinant prostasin to the basolateral side of polarized Caco-2 monolayers causes matriptase activation and stimulates barrier formation that is dependent upon expression of matriptase (31). Hence, prostasin acts upstream of matriptase, and matriptase is the effector protease that directly enhances barrier function. Consistent with this role in intestinal barrier protection, rats possessing a natural homozygous mutation in the prostasin gene that causes reduced proteolytic activity show increased susceptibility to DSS-induced colitis (37, 38).

The regulation of the matriptase-prostasin axis in intestinal epithelium and during inflammatory colitis is not known. We hypothesized that cytokine-dependent intestinal barrier permeability could be associated with the down-regulation of matriptase and/or prostasin. Using the experimental model of DSS-induced colitis in mice, here we show that both matriptase and prostasin are transcriptionally down-regulated during the initiating phase of experimental colitis, and that the loss of these proteases precedes the appearance of clinical symptoms. The data suggest that inflammatory cytokine-mediated down-regulation of these proteases could contribute significantly to disease susceptibility and progression.

Results

The early response to experimental colitis is similar between control and St14 hypomorphic mice

DSS administered via drinking water induces a form of colitis in mice with features similar to those found in human UC (39). The initiating trigger, DSS, causes injury to the epithelial layer, provoking activation of an innate immune response to luminal contents. Treatment of mice with 2% DSS in drinking water for 7 days followed by removal of the DSS stimulus at day 8, results in intestinal injury with increasing clinical symptoms of acute colitis characterized by bloody diarrhea, ulcerations, and inflammatory infiltrates that reach maximum at 7–8 days. Removal of the DSS at day 8 results in rapid mucosal recovery that is associated with a progressive reduction of clinical symptoms. In previous studies we found that, unlike wild-type littermate control mice, *St14* hypomorphic mice fail to recover from DSS-induced injury after removal of the DSS, with progression in the severity of clinical symptoms and hastened mortality (30). Given the enhanced intestinal barrier permeability in the *St14* hypomorphic mice compared with their wild-type littermates (30), it was unclear why their initial response to DSS appeared so similar. To investigate this initial phase in more detail, 2% DSS was administered to *St14* hypomorphic and control littermate mice in drinking water for up to 5 days and the regulation of matriptase investigated.

The shorter duration of DSS treatment reduced the aggravation of symptoms and enhanced survival of the *St14* hypomorphic mice. The body weights of both the *St14* hypomorphic and control groups remained relatively constant through the 5 days of DSS treatment, with weight loss starting to be apparent only at day 5 (Fig. 1*A*). The *St14* hypomorphic mice developed clinical symptoms similar to control mice, including shortening of colon length (an indicator of colonic inflammation) (Fig. 1*B*) and increased spleen weight (an indicator of systemic inflammation) (Fig. 1*C*). Likewise, the overall clinical disease score, a combination of weight loss, stool consistency, and blood in stool, was similar in both groups and was not significant until day 5 (Fig. 1*D*); however, there was a trend toward enhanced clinical symptoms in *St14* hypomorphs compared with littermate controls at day 1.5 (Fig. 1*D*). Consistent with this, the distal colonic segments from *St14* hypomorphic mice treated with DSS for 1.5 days microscopically appeared mostly normal (Fig. 1*E*, *middle panels, 20*×) but displayed a few areas of patchy damage, whereas at day 5 both groups had a similar level of damage, immune infiltration, and loss of colonic mucosa (Fig. 1*E*, *right panels*), compared with water-alone treated mice (Fig. 1*E*, *left panels*).

The onset of clinical symptoms during acute experimental colitis correlates with decreased matriptase and prostasin expression

Matriptase and prostasin protein expression during experimental colitis was examined by immunohistochemical staining of colonic epithelium. In control mice, strong matriptase

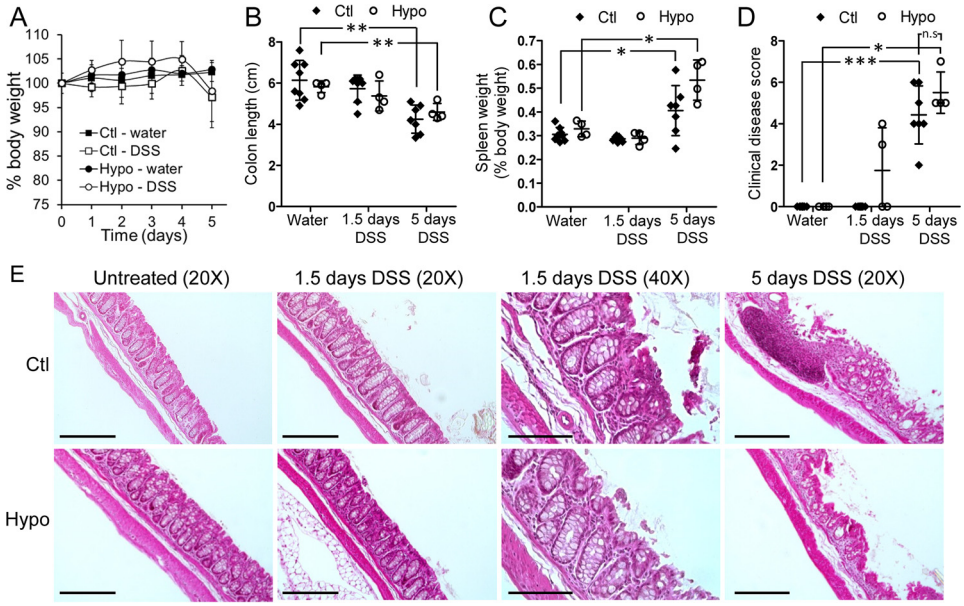

Figure 1. Clinical symptoms induced during the initiating phase of murine colitis do not become significant until 5 days of DSS treatment in littermate control and *St14* hypomorph mice. *St14* hypomorph (*Hypo*) mice and littermate control (*Ctl*) mice were treated with 2% DSS in drinking water or water alone. *A*, body weight was monitored daily and expressed relative to day 0, mean ± S.D. ($n = 4–6$ per group). *B*, colon lengths measured in littermate controls and *St14* hypomorph mice after sacrifice at the indicated times after DSS treatment (Ctl, $n = 7–8$/group; Hypo, $n = 4$/group). Colon lengths are significantly shorter after 5 days' DSS treatment compared with mice treated with water alone. **, $p < 0.01$, unpaired *t* test. *C*, spleen weights (expressed as % body weight, mean ± S.D.) are significantly higher after 5 days' DSS treatment in both groups. *, $p < 0.05$, Mann-Whitney *U* test (Ctl, $n = 7–8$/group; Hypo, $n = 4$/group). *D*, clinical disease scores mean ± S.D. (Ctl, $n = 7–8$/group; Hypo, $n = 4$/group). Both groups do not show significant clinical disease until day 5. ***, $p < 0.001$, *, $p < 0.05$, Mann-Whitney *U* test. *E*, representative H&E-stained images of distal colons from *St14* hypomorph and littermate control mice at the indicated times of DSS treatment. The majority of tissue after 1.5 days' treatment appears normal with some patchy damage (*middle panels*, *20×*, *40×*), but extensive damage was evident at day 5 with immune cell infiltrate and loss of colonic villi. *Scale bars*: 20× = 200 μm, 40× = 100 μm.

staining was localized to colonic epithelial cells, with expression levels increasing from colonic crypts toward villous tips (Fig. 2*A, 200×*). Higher-magnification images show that matriptase is concentrated at epithelial junctions of the murine colonic villi (Fig. 2*A*, *600×*, *arrow*), which is consistent with its observed expression in polarized human colonic epithelium (29, 40). Prostasin is similarly expressed most highly at villous tips (Fig. 2*B, 200×*), but displays a more diffuse and apical location in villous epithelial cells (Fig. 2*B, 600×*, *arrow*), a pattern similar to its localization in human colonic epithelium and other epithelial tissues (41–43). After administration of DSS for 5 days, expression of both matriptase and prostasin in the colonic tissues was dramatically decreased compared with water alone (Fig. 2). Reduced staining for both matriptase and prostasin was observed in areas of colonic injury as well as in areas where the epithelium appeared to remain intact, as visualized by β-tubulin staining. Both matriptase and prostasin were consistently reduced at the villous tips, with prostasin expression appearing to be particularly reduced on the apical surface (Fig. 2, *A* and *B*, *200×*, *600×*). Quantitation of staining intensities using image analysis software showed that matriptase and prostasin protein expression are significantly decreased by ~2-fold and ~4-fold, respectively, in the colonic epithelium of mice exposed to DSS (Fig. 2*C*).

Together, these data indicate that the similarity in clinical symptoms between matriptase-sufficient control mice and *St14* hypomorphic mice during the initial response to DSS may be explained by the down-regulation of matriptase and prostasin in control mice after treatment with DSS.

Matriptase and prostasin mRNA levels are decreased early in experimental colitis

To better understand the mechanisms responsible for the down-regulation of matriptase in colonic epithelium after exposure to DSS, matriptase and prostasin mRNA levels were determined by quantitative PCR (qPCR) analysis of colonic epithelial tissues isolated from control mice administered DSS for either 1.5 or 5 days. The mRNA expression was normalized to the mRNA of the epithelial cell marker EpCAM to account for the possible loss of signal because of epithelial cell death by DSS exposure (Fig. 3, *A* and *B*). Both matriptase and prostasin mRNA levels were significantly decreased as early as 1.5 days after DSS administration and remained low through 5 days of DSS treatment, compared with mice treated with water alone (Fig. 3, *A* and *B*). The down-regulation of both protease mRNAs occurs before the appearance of significant clinical symptoms (Fig. 1, *A–D*), consistent with the notion that loss of this pathway contributes to the pathogenesis of colitis.

St14 gene transcription is down-regulated during experimental colitis

qPCR of mRNA measures the steady state levels of mRNA transcripts, which are a combination of gene transcription rates and post-transcriptional regulatory mechanisms. To determine whether *St14* gene activity is down-regulated in colonic epithelium exposed to DSS, we analyzed promoter-driven gene expression *in vivo* utilizing the heterozygous *St14* hypomorphic mouse strain, which harbors an ST14 allele containing a β-galactosidase gene trap (GT) under the control of the ST14 pro-

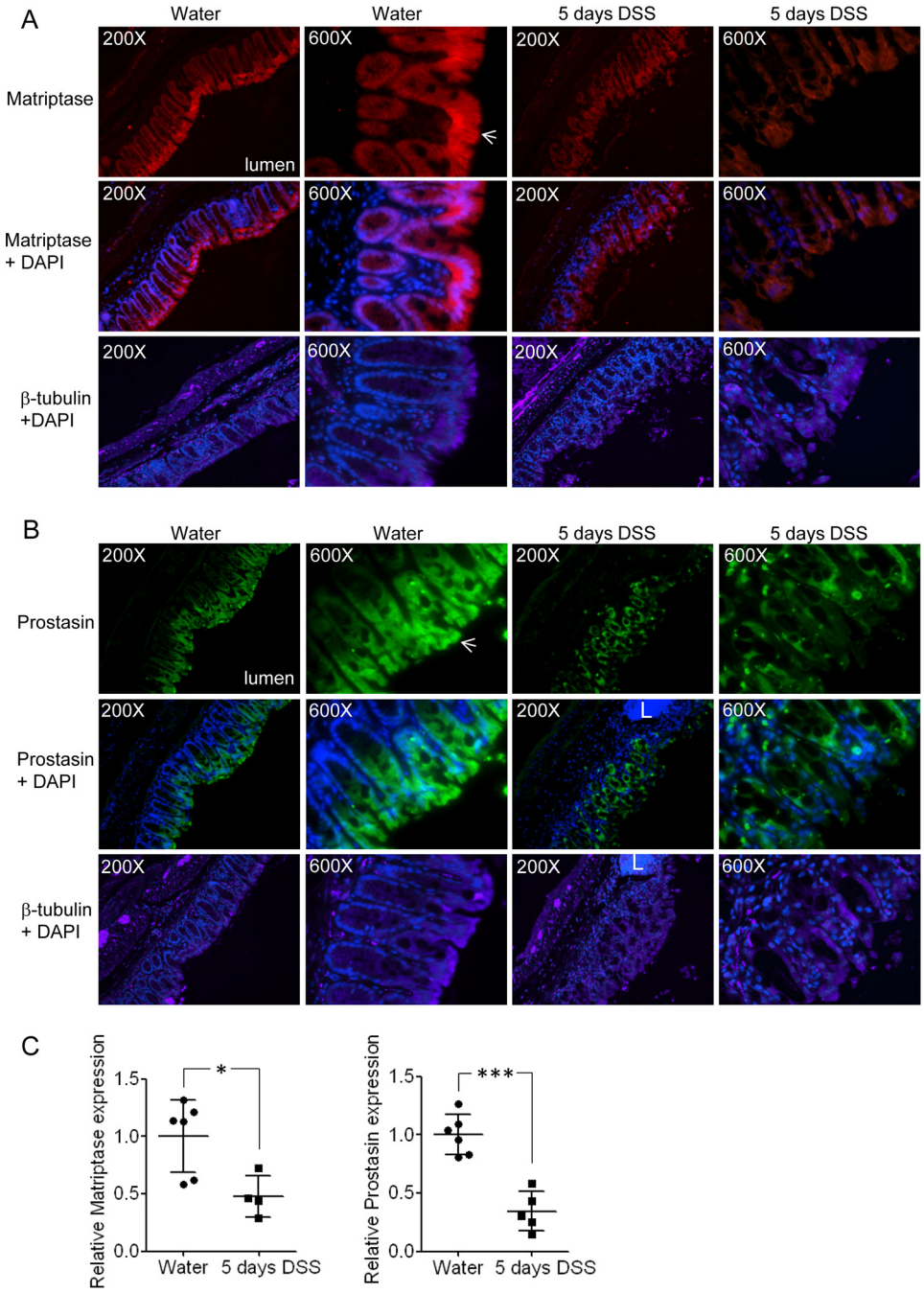

Figure 2. Matriptase and prostasin proteins are significantly down-regulated during murine colitis. *A* and *B*, representative immunostaining of distal colon sections from untreated control mice or after 5 days of DSS treatment. Images from different treatment groups were captured at equal exposure times and are shown at 200× or 600×. In untreated mice both proteases are most highly expressed at villous tips, matriptase concentrates at epithelial cell junctions (*A*, *water*, *600×*, *arrow*), whereas prostasin displays a more diffuse and apical distribution (*B*, *water*, *600×*, *arrow*). DSS treatment causes a reduction in staining intensity for both proteases, with evidence of leukocyte infiltrate (*L*) in some colonic segments of DSS-treated mice. β-tubulin staining of similar regions of colonic sections shows the epithelial cells, where matriptase and prostasin expression is reduced. *C*, quantitation of signal intensities of matriptase and prostasin in colons sections from untreated or DSS-treated mice ($n = 4–6$ mice/group). Graphs show mean ± S.D. *, $p < 0.05$, ***, $p < 0.001$, unpaired *t* test.

moter (44, 45). Although these mice express 50–55% of normal matriptase levels, their intestinal epithelial barrier function is normal compared with littermate control mice (30).[3] β-galactosidase activity as measured by hydrolysis of X-gal was used to monitor *St14* promoter-driven gene expression. Comparison of X-gal staining of colonic tissues from heterozygous *St14* hypomorphic mice administered DSS for either 1.5 or 5 days, or water alone, shows a dramatic loss in the intensity of blue staining in the presence of DSS, even in areas where the intestinal epithelium remains intact (Fig. 3*C*, *40×*). These data show that mucosal inflammation induced by exposure to DSS down-regulates matriptase through suppression of the *St14* gene promoter.

[3] S. Netzel-Arnett, M. S. Buzza, T. Shea-Donohue, and T. M. Antalis, unpublished data.

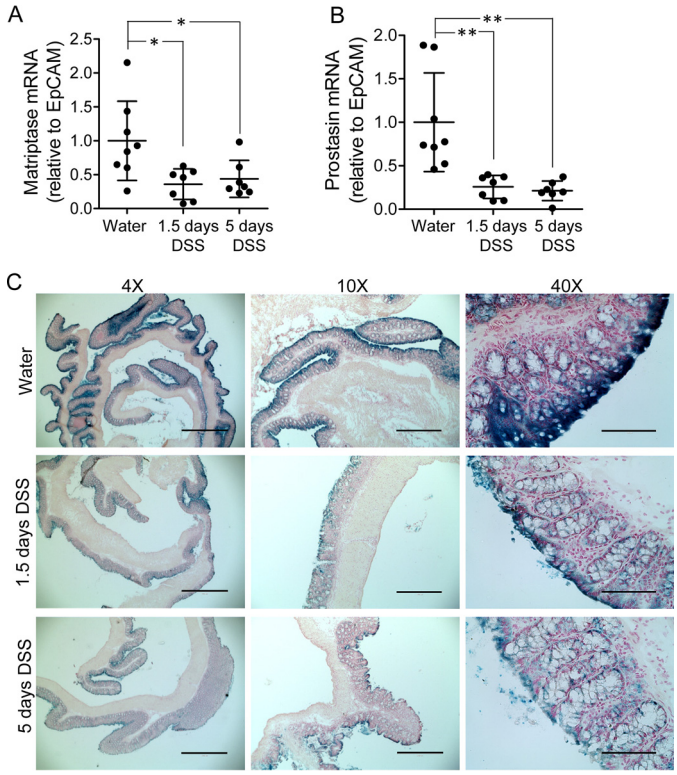

Figure 3. Matriptase and prostasin mRNA are down-regulated early during the initiating phase of murine colitis. *A* and *B*, qPCR analysis of mRNA isolated from control mice after treatment with 2% DSS for 1.5 or 5 days for matriptase (*A*) and prostasin (*B*). Signals were first normalized to GAPDH to account for cDNA content, and then normalized to the epithelial marker EpCAM. mRNA for both proteases is significantly down-regulated at both 1.5 days and 5 days of DSS treatment ($n = 6–8$ mice/group). Graphs show individual mice in each treatment group, and mean ± S.D. *, $p < 0.05$, **, $p < 0.01$, unpaired *t* test. *C*, X-gal staining (*blue*) of proximal colons from littermate control mice treated with water alone compared with DSS-treated mice. Representative images from 6–8 mice/group. *Scale bars*: 4× = 1000 μm, 10× = 400 μm, 40× = 100 μm.

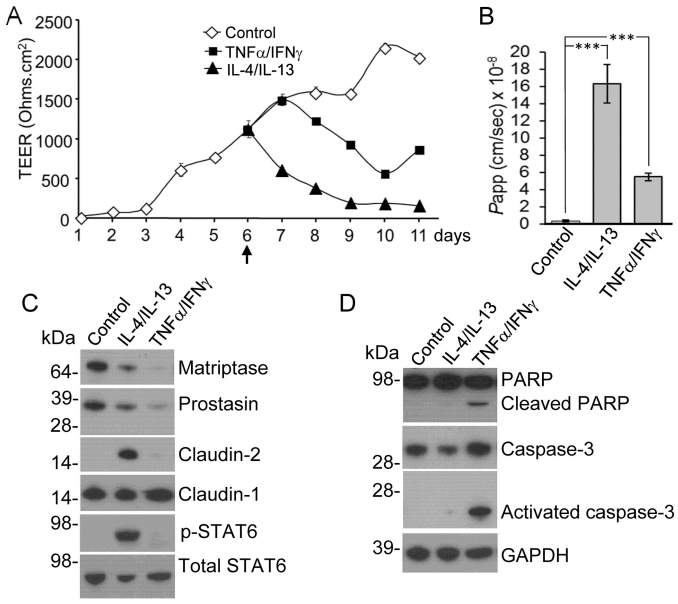

Figure 4. Cytokines that are implicated in UC down-regulate matriptase and prostasin during disruption of polarized T84 epithelial barriers. T84 cells were plated onto Transwell filters and allowed to develop barrier function for 6 days as assessed by TEER, and were then treated basolaterally with 10 ng/ml of the indicated cytokines for 5 days (*arrow below A*). *A*, addition of both combinations of cytokines decreased TEER over time, mean ± S.E. from triplicate wells. Data are representative of two experiments. *B*, measurement of the paracellular permeability of T84 monolayers to 4 kDa FITC-dextran assessed after 5 days of cytokine treatment (day 11 in *A*), shows a significant disruption of epithelial barrier function by both combinations of cytokines, mean ± S.E. from quadruplicate wells. ***, $p < 0.001$, unpaired *t* test. *C* and *D*, immunoblot analysis of whole cell lysates prepared on day 5 of cytokine treatment (day 11 in *A*) probed with the indicated antibodies. Data show decreased matriptase and prostasin expression, elevated claudin-2, increased STAT6 activation (*p-STAT6*, phospho-STAT6) induced by IL-4 and IL-13, and increased apoptosis induced by TNFα and IFNγ. Data are representative of two independent experiments.

Th2 cytokines down-regulate the prostasin-matriptase pathway and are associated with increased epithelial barrier permeability

The colonic mucosa of UC patients maintains a Th2-like cytokine pattern (10). To model the effect of Th2 cytokines implicated in UC on matriptase and prostasin expression and epithelial permeability, we utilized polarized human colonic epithelial T84 monolayers, which we have shown previously to be dependent on matriptase expression for barrier formation (30). T84 monolayers were cultured on Transwell filters for 6 days until well polarized (transepithelial electrical resistance (TEER) of >1000 ohms·cm^2), and were then treated basolaterally with Th2 cytokines (IL-4 and IL-13) or Th1 cytokines (TNFα and IFNγ) for comparison (Fig. 4). Both combinations of Th1 and Th2 cytokines disrupted the epithelial barrier over 5 days, as demonstrated by the decrease in TEER (Fig. 4*A*) and by the significant increase in paracellular permeability to 4 kDa FITC-dextran (Fig. 4*B*), consistent with previous reports (13).

Both matriptase and prostasin protein expression were substantially decreased by both combinations of cytokine treatments at day 5 after cytokine treatment (Fig. 4*C*). IL-13 and IL-4 mediate their activities by binding to a dimeric receptor, which triggers signaling cascades leading to the phosphorylation of signal transducer and activation of transcription 6 (STAT6) and downstream gene regulation (46). The Th2 cytokines induced the activation of STAT6, as indicated by the increased levels of phospho-STAT6 (p-STAT6) (Fig. 4*C*). Claudin-2 was also induced by the Th2 cytokines, which has been correlated previously with loss of matriptase and/or prostasin in Caco-2 intestinal epithelium and in the colonic epithelium of *St14* hypomorphic mice (29–31). Although IL-13 has been reported to induce apoptosis in human intestinal epithelial HT29 monolayers (8, 47), we did not detect an increase in the apoptosis markers, cleaved PARP, or activated caspase-3 after treatment with the Th2 cytokines. In contrast, the Th1 cytokines, which also decreased matriptase and prostasin protein expression, were associated with induction of these apoptotic markers (Fig. 4, *C* and *D*), indicating that apoptosis likely contributes to the Th1 cytokine-induced barrier permeability. These data show that the induction of T84 barrier permeability by the Th2 cytokines IL-4 and IL-13 is not dependent on cell death but instead suggest that the increased barrier permeability and enhanced claudin-2 expression are caused by Th2 cytokine-induced loss of the matriptase-prostasin barrier-protective pathway.

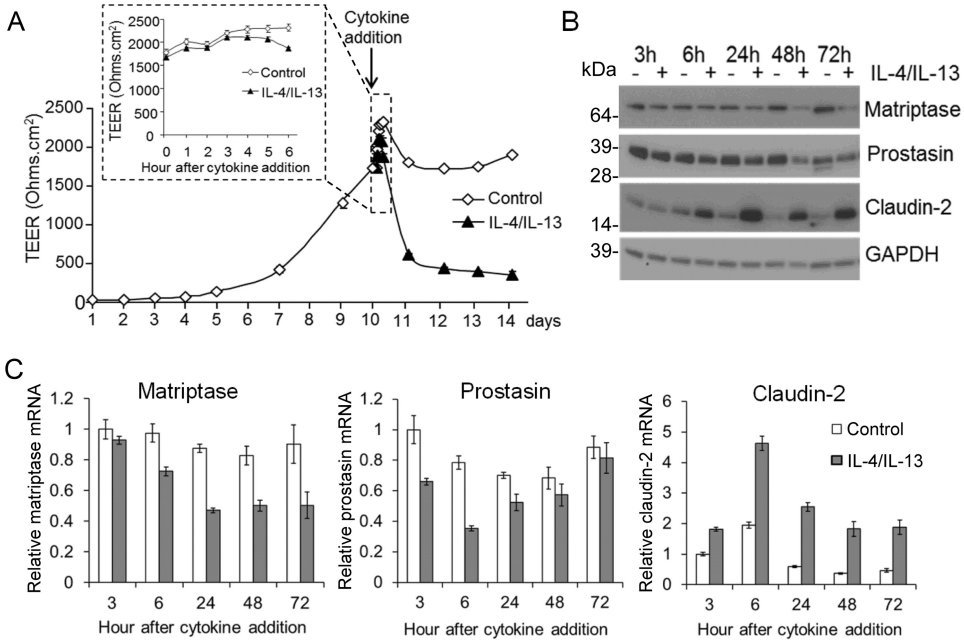

Figure 5. IL-4/IL-13 induce time-dependent down-regulation of matriptase and prostasin. T84 monolayers were allowed to develop barrier function for 10 days, at which time they were treated basolaterally with 10 ng/ml IL-4 and IL-13 (*arrow*) for 5 days. *A*, measurement of TEER shows that cytokine-induced TEER loss begins at ~6 h of treatment (*inset*). Graphs show mean ± S.E. from triplicate wells. Data are representative of two experiments. *B*, immunoblot analysis of whole cell lysates prepared at the indicated times after cytokine addition show both matriptase and prostasin protein levels start to decrease after 24 h of treatment. Matriptase expression remains suppressed over 72 h, whereas prostasin expression returns at 72 h. *C*, qPCR analysis of matriptase, prostasin, and claudin-2 mRNA expression in IL-4/IL-13 treated T84 monolayers compared with untreated monolayers. Signals were normalized to GAPDH and expressed relative to untreated at 3 h. Matriptase mRNA is significantly lower after 24 h of treatment ($p < 0.001$) and remains suppressed over 72 h, whereas prostasin mRNA is significantly lost by 6 h ($p < 0.05$) but begins to return at 24 h (n.s). Data are representative of two independent experiments, from triplicate wells each.

Time-dependent down-regulation of matriptase and prostasin in human colonic T84 epithelium during Th2-mediated barrier disruption

To gain insight into the time-dependent regulation of matriptase and prostasin expression relative to the loss of barrier function, a time course analysis of barrier disruption by the Th2 cytokines in T84 monolayers was performed (Fig. 5). TEER measurements showed that barrier disruption is clearly apparent at ~6 h after the addition of cytokines (Fig. 5*A*) and is associated with an increase in claudin-2 protein expression through 72 h (Fig. 5*B*). Matriptase and prostasin protein levels start to decrease at the 24 h time point, and whereas matriptase remains low through 72 h, prostasin levels are decreased at 48 h and recover by 72 h (Fig. 5*B*).

The decrease in matriptase and prostasin also occurs at the mRNA level, with loss of both mRNAs beginning around 6 h after cytokine addition (Fig. 5*C*), correlating with barrier disruption and increased claudin-2 mRNA expression at the same time point. Matriptase mRNA remains suppressed over the course of the experiment through 72 h, matching its protein expression (Fig. 5, *B* and *C*), whereas prostasin mRNA expression begins to return after 24 h, and returns to normal levels by 72 h. These data suggest that the mRNA levels of these proteases are differentially regulated by Th2 cytokines.

Claudin-2 mRNA is rapidly induced in response to Th2 cytokine treatment (Fig. 5*C*), consistent with published reports (17). By 48 h the induced claudin-2 mRNA expression has returned to close to initial levels, yet the claudin-2 protein levels remain high through 72 h. (Fig. 5*B*). The loss of matriptase protein and the increased claudin-2 protein levels at 48–72 h is likely because of the promotion of claudin-2 turnover by matriptase, as we have reported previously (29). These data suggest that Th2 cytokines initiate a barrier-disruptive pathway that involves coordinated dysregulation of both claudin-2 and the matriptase-prostasin pathway.

Th2 cytokine-induced down-regulation of matriptase is rescued by the STAT6 inhibitor SAHA

Together these data suggest that Th2 cytokines induce the down-regulation of matriptase though a mechanism that involves activation of STAT6 (Fig. 4*C*), which contributes to epithelial barrier disruption. SAHA (suberoylanilide hydroxamic acid) is a histone deacetylase (HDAC) inhibitor that prevents the phosphorylation and activation of STAT6 by IL-4 and IL-13 (47). We found that the addition of SAHA inhibited the Th2 cytokine-induced loss of TEER at 6 and 24 h, and the up-regulation of claudin-2 mRNA and protein (Fig. 6, *A* and *B*). SAHA also prevented the down-regulation of matriptase mRNA levels by the Th2 cytokines at 24 h, and the down-regulation of prostasin mRNA at 6 h (Fig. 6*A*). Immunoblot analysis confirmed the decrease in Th2 cytokine-mediated phosphorylation of STAT6 in the presence of SAHA (Fig. 6*B*). The decrease in matriptase protein expression after 24 h of Th2 cytokine treatment is also rescued when cells are exposed to SAHA (Fig. 6*B*). Similar results were observed when STAT6 was knocked down by siRNA silencing (supplemental Fig. S1). Together these data suggest that matriptase and prostasin down-regulation in colonic epithelium is regulated by Th2-mediated STAT6 activation and signaling.

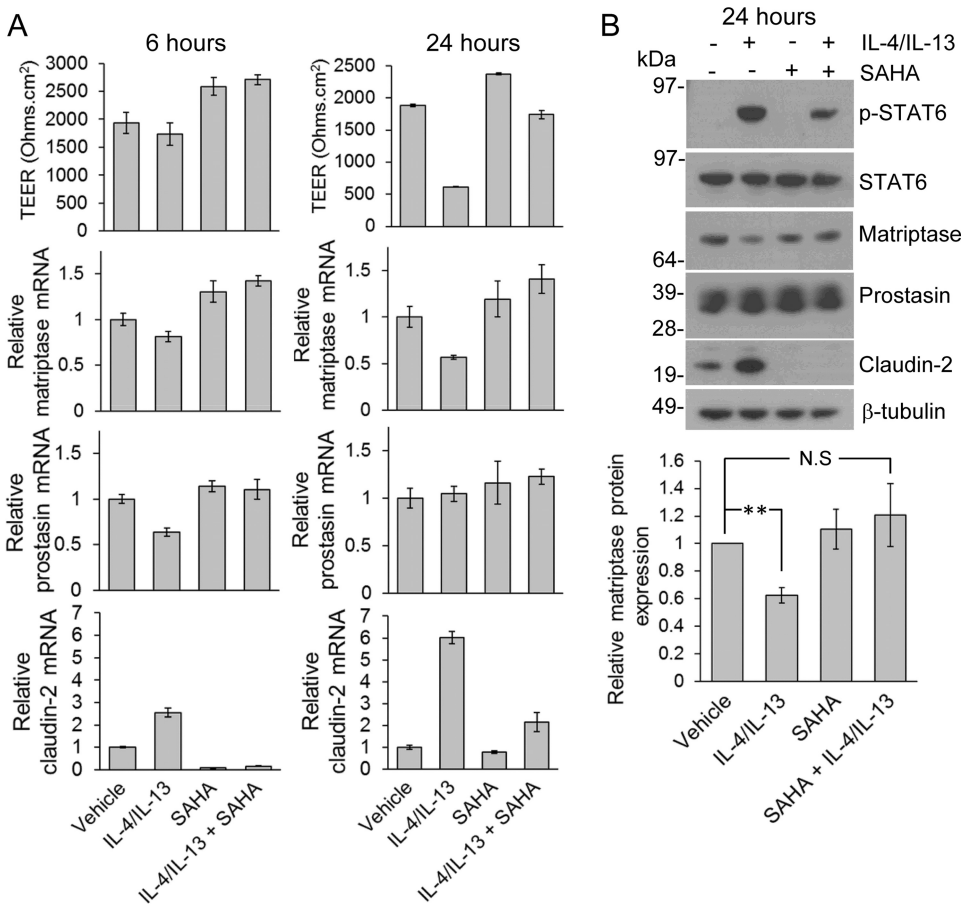

Figure 6. The STAT6 inhibitor SAHA prevents the loss of barrier function and down-regulation of matriptase and prostasin mRNA induced by IL-4/IL-13. Polarized T84 monolayers on Transwell filters were treated basolaterally with 10 ng/ml each IL-4 and IL-13 with or without pretreatment with 5 μM SAHA for 1 h. *A*, analysis of TEER and matriptase, prostasin, and claudin-2 mRNA expression at 6 and 24 h after cytokine addition. Both TEER and matriptase mRNA expression are significantly decreased by 24 h of treatment with IL-4/IL-13 ($p < 0.05$), which is abrogated in the presence of SAHA. The significant loss of prostasin mRNA that occurs at 6 h in the presence of IL-4/IL-13 ($p < 0.001$) is also inhibited by SAHA. Signals are normalized to 18S rRNA because we found GAPDH mRNA to be regulated by SAHA. Data are representative of three independent experiments. Mean ± S.E. *B*, immunoblots of whole cell lysates at 24 h (*top*) and densitometry analysis of matriptase protein expression (*bottom*). The data show a decrease in IL-4/IL-13 induced STAT6 phosphorylation, the prevention of loss of matriptase protein, and the failure to upregulate claudin-2 in the presence of cytokines by SAHA. The *bottom panel* shows a significant loss of matriptase protein that is recovered in the presence of SAHA as quantified by densitometry. Matriptase protein expression is expressed relative to vehicle-treated cells after normalizing to β-tubulin at 24 h of treatment. Graph shows mean ± S.E. from three independent experiments. **, $p < 0.01$, unpaired *t* test.

The matriptase-prostasin proteolytic axis is down-regulated in human IBD colonic tissues

Mucosal inflammation during UC is associated with elevated Th2 cytokines (9, 19, 20). To determine whether the matriptase-prostasin pathway is altered during human colitis, a cDNA microarray of human colonic tissues from normal, ulcerative colitis and Crohn's disease patients was analyzed for prostasin and matriptase expression. The mRNA signals were normalized to the epithelial cell marker EpCAM, in consideration of the variation in epithelial cell content of individual tissue samples. We found that matriptase and prostasin mRNA levels are significantly reduced in colonic tissues from patients with both UC and CD (Fig. 7), consistent with the loss of this barrier-protective protease pathway in the dysregulation of barrier function during human IBD.

Discussion

The prostasin-matriptase axis plays a key role in the regulation and maintenance of epithelial barrier function (28, 31, 48, 49). Here, we show that the coordinate down-regulation of matriptase and prostasin by cytokines produced during inflammatory colitis likely contributes to the increased permeability associated with cytokine-mediated intestinal epithelial barrier dysfunction during colitis. Down-regulation of these proteases occurs early in the initiating phase of inflammatory experimental colitis in mice, prior to the appearance of clinical symptoms, suggesting that the loss of this protease axis plays a key role in disease susceptibility.

The dramatic and early loss of matriptase and prostasin mRNA in murine colonic tissue during DSS-induced colitis suggests that even low levels of inflammation can cause the loss of this barrier-protective pathway, therefore perpetuating disease progression. The early mRNA down-regulation also indicated that that this protease pathway may be directly regulated by inflammation, which was confirmed using the *St14* β-galactosidase reporter mice, which showed a clear loss of matriptase gene transcription during inflammatory colitis. Our *in vitro* studies using polarized human T84 epithelial cells confirmed that Th2 inflammatory cytokines induce the down-regulation of matriptase and prostasin protein as well as mRNA expression. Interestingly cytokine-induced down-regulation of

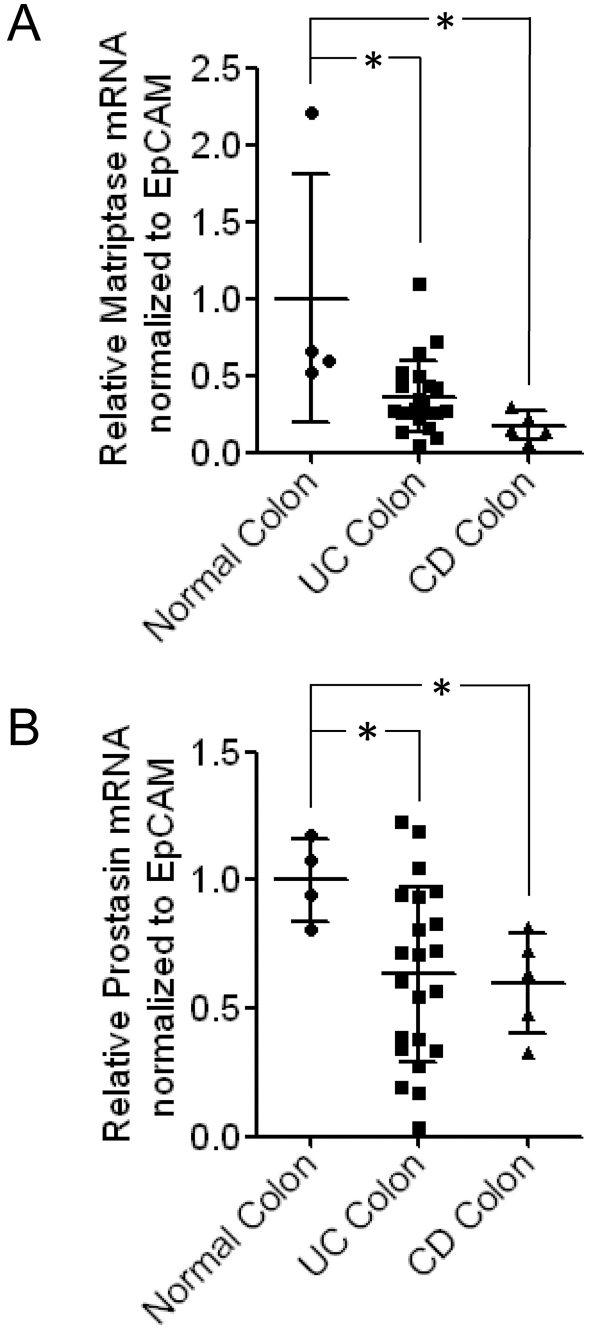

Figure 7. Matriptase and prostasin are significantly decreased in colonic epithelium of human IBD patients. *A* and *B*, the TissueScan Crohn's and Colitis Tissue qPCR Panel II was analyzed for matriptase (*A*) and prostasin (*B*) expression by qPCR. Signals were normalized to β-actin mRNA and then normalized to EpCAM mRNA to account for variation in epithelial content of individual samples. Graphs show mean $\pm$ S.D. *, $p < 0.05$, unpaired *t* test.

matriptase and prostasin was dependent on the formation of a polarized T84 epithelial barrier, which is achieved by plating the epithelial cells on Transwell filters and allowing differentiation with TEER development, wherein they resemble colonic epithelium. Even so, the induced protease mRNA loss did not appear as dramatic *in vitro* as observed *in vivo*, which may reflect a more complex milieu of cytokines induced during colitis. Th1 cytokines also induced the loss of matriptase and prostasin protein *in vitro*, which is consistent with studies by others showing that matriptase loss in psoriatic skin lesions is regulated by TNFα via an IKK2/NFκB signaling pathway (50).

To date, there has not been a thorough examination of either the matriptase or prostasin promoter to identify elements that may regulate their expression. Our data suggest that Th2-induced matriptase down-regulation occurs at the gene expression level through the activity of STAT6. It is possible that matriptase gene expression is suppressed indirectly after Th2 cytokine-induced STAT6 activation, because STAT6 can both induce direct gene transcription and indirectly negatively regulate gene expression presumably via the induction of transcriptional repressors (51). Our previous studies showed that prostasin functions upstream of matriptase to stimulate intestinal epithelial barrier formation (31). An interesting finding from this study is that although they are down-regulated, they do not follow the same pattern. Matriptase expression remains suppressed in the presence of Th2 cytokines, however prostasin mRNA and protein loss appears more transient. This re-expression of prostasin may represent a feedback loop where the increase in prostasin serves to activate matriptase in an attempt to reform the epithelial barrier.

It is also possible that post-translational regulation could contribute to protease down-regulation, because the loss of protein expression occurs after barrier disruption in the *in vitro* model. In T84 and Caco-2 monolayers, we have found that matriptase and prostasin protein levels correlate with barrier tightness, which is not reflected in a corresponding increase in mRNA levels (29, 31),[4] and intact cell junctions are required for matriptase expression at epithelial adherens junctions (52). It is possible that cytokine-induced alteration of adherens junctions could stimulate matriptase endocytosis and degradation via mechanisms similar to other junctional proteins such as E-cadherin with which matriptase is co-localized (29, 53, 54).

The *in vitro* studies using T84 monolayers demonstrate that the Th2 cytokines IL-13 and IL-4, whose activity is associated with elevated claudin-2 expression, induce the down-regulation of matriptase and prostasin through activation of STAT6. Epithelial STAT6 phosphorylation is elevated in patients with UC (47), and inhibition of STAT6 expression or activation is sufficient to prevent IL-13-induced epithelial barrier disruption, and to ameliorate the severity of colitis in murine models (17, 47, 55–57).

Cell surface claudin-2 inserts into epithelial tight junctions to form paracellular pores that mediate the transport of sodium, potassium, and water via a leak flux mechanism, contributing to diarrhea in IBD (58–60). Our data suggest that in addition to the regulation of claudin composition at the tight junctions, Th2 cytokines initiate a coordinate program that also leads to the loss of the matriptase-prostasin pathway which not only mediates the post-translational turnover of claudin-2, but also causes increased macromolecular permeability in intestinal epithelium through mechanisms that are as yet unclear. Pharmacological inhibition of STAT6 with SAHA restores protease expression and reverses cytokine-induced barrier dysfunction including the induced expression of claudin-2. These data sug-

[4] M. S. Buzza and T. M. Antalis, unpublished data.

gest that preventing the loss of the matriptase-prostasin axis in IBD using HDAC inhibitors may represent a viable treatment strategy for uncontrolled disease. HDAC inhibitors such as SAHA (also known as vorinostat) are under investigation for the treatment of other inflammatory conditions and malignancies and have been FDA approved for treatment of T-cell lymphoma (61, 62). Their successful use in several murine colitis models suggests they may offer a potential therapeutic benefit for IBD patients (63).

The regulation of intestinal permeability is a delicate balance, because the intestinal epithelial barrier regulates the paracellular transport of water, ions, and nutrients while providing a barrier to microbial translocation. Our data demonstrate that inflammatory cytokines disrupt barrier function, mediated in part by down-regulation of epithelial matriptase and prostasin that, in turn, propagates an inflammatory cycle and enhances the severity of colitis. The loss of gene expression occurs before the onset of clinical symptoms which may promote disease initiation. Thus, targeting the enhancement of the prostasin-matriptase axis, or preventing its loss, may be therapeutically effective, particularly in inhibiting the reactivation of quiescent IBD.

Experimental procedures

DSS-induced experimental colitis in mice

These studies utilized the *St14* hypomorphic mouse strain (provided by T. Bugge, NIH) and their littermate controls which have been described previously (44, 64). *St14* hypomorphic mice possess one *St14* null allele and one allelle in which a β-galactosidase reporter has been inserted into the matriptase locus (GT allele). This allele still undergoes a low level of full-length matriptase transcription, so that the mice express 1–5% of normal matriptase levels. Littermate control mice contain one wild-type matriptase allele and either a GT allele or a null allele, and were used for the majority of the studies. These mice express 50–55% of normal matriptase levels and show no difference in susceptibility to DSS-induced colitis compared with wild-type C57BL/6J mice (30). To induce inflammatory colitis, adult mice (8–12 weeks old, male and female) were administered 2% (w/v) DSS (molecular weight of 36,000–50,000) (MP Biomedicals, lot number, M5975) in drinking water for 1.5 or 5 days or were given water only. Mice were weighed daily and a clinical disease score on (a scale of 1–5) was quantified based on the sum of weight loss, stool consistency, and fecal occult blood (guaiac test, Sure-Vue, Thermo Fisher). All mice were bred and housed in the University of Maryland Baltimore animal facility, so that they were expected to have the same level of environmental exposure to microbes. Animal care and experimental procedures were approved by the University of Maryland School of Medicine Institutional Animal Care and Use Committee (IACUC).

Tissue analysis

Gastrointestinal tracts from mice treated with water alone or after 1.5 or 5 days' treatment with DSS were removed and colon lengths (anus to cecum) documented. Spleen weights were recorded as an indicator of inflammation. 1-cm colon segments were dissected and identical tissue segments from each mouse were compared for molecular analyses. Tissues were either (*a*) fixed in 4% paraformaldehyde (PFA; distal colon), paraffin embedded, cut into 5-μm sections, and sections stained with H&E or used for immunohistochemical staining for matriptase and prostasin; (*b*) frozen in OCT after preparation using the "Swiss roll" technique (65) (proximal colon) and used for X-gal staining as described below; or (*c*) snap frozen for preparation of RNA for qPCR analyses (distal colon). Immune infiltration was quantified based on a combined score of inflammatory cell infiltrate (range 0–4) and extent of inflammatory cell infiltrate (range 0–3) along the length of each H&E-stained tissue segment as in Ref.30.

Immunohistochemical detection of matriptase and prostasin expression

Heat-induced antigen retrieval in 10 mM citrate buffer was performed on colonic tissue sections fixed in 4% PFA. Sections were stained with 0.5 μg/ml sheep anti-matriptase antibody (R&D Systems), and detected using anti-sheep DyLight594 secondary antibody (Thermo Fisher). The specificity of matriptase staining was validated using *St14* hypomorph colonic sections which showed substantially reduced staining intensity compared with control mice (data not shown), and as observed by others using *St14* ablated tissues (40). Prostasin was detected using mouse anti-prostasin antibody (0.5 μg/ml) (BD Biosciences) and visualized with goat anti-mouse Alexa Fluor 488 secondary antibody (Life Technologies) after blocking using the Vectastain M.O.M. kit (Vector Laboratories). Colonic cells were visualized using β-tubulin, using rabbit anti-β-tubulin antibody (2 μg/ml) (Santa Cruz Biotechnology), detected with goat anti-rabbit Alexa Fluor 647 secondary antibody (Life Technologies). Nuclei were counterstained using DAPI. For quantitation, images of protease staining were captured from two or three 20× fields per colon (depending on section size) using Volocity Image Analysis Software, with equal exposure time set for all samples for each antibody. Signal intensities (average pixels/field) were determined using ImageJ analysis software from at least 2 × 300 μm^2 areas for each 20× field, setting an identical threshold for all samples for each antibody. The average pixels/field for the water alone control compared with DSS-treated colonic tissues was calculated, and levels expressed relative to the average control signals.

X-gal staining of frozen colonic tissue sections

Frozen sections were stained with X-gal using a β-galactosidase staining kit (Mirus Bio), according to manufacturer's instructions. Briefly, sections were fixed then incubated with X-gal solution at 37 °C for 16 h in a humidified chamber. After color development, sections were counterstained using nuclear fast red. Images were captured using an EVOS FL Auto microscope (Life Technologies) at the indicated magnifications.

Cell culture, cytokine treatment, and measurement of monolayer permeability

T84 cells were cultured and plated as described previously (30). For barrier development, cells were plated on 1.12-cm^2 Transwell filters (Costar) at 3 × 10^5 cells/well and allowed to become confluent and polarize over 7–10 days. Barrier function was assessed daily through the measurement of TEER using an EVOM voltohmmeter with chopstick probes as described (29).

Cytokine treatments were performed after cultures had reached a TEER of >1000 ohms·cm^2. Recombinant human TNFα, IFNγ, IL-4, or IL-13 (Peprotech) (10 ng/ml each) was added to the basolateral chamber, and cytokine containing media replaced daily. In some experiments cultures were pretreated with 5 μM SAHA or DMSO vehicle for 1 h prior to the addition of cytokines. Assessment of paracellular permeability to macromolecules was performed using 4 kDa FITC-conjugated dextran, and the apparent monolayer permeability calculated as described (29).

Cell lysis and immunoblotting

T84 monolayers were lysed in LDS sample buffer (Life Technologies) containing reducing agent, and after homogenization, equal volumes of lysate were resolved by SDS-PAGE, and immunoblotted as described (29). Equivalent protein loading per lane is demonstrated by immunoblotting for GAPDH or β-tubulin as indicated. Membranes were sequentially probed with the following antibodies: rabbit anti-matriptase (IM1014, Calbiochem), mouse anti-prostasin (612172, BD Biosciences), rabbit anti-claudin-2 (51–6100, Invitrogen), rabbit anti-claudin-1 (71–7800, Invitrogen), rabbit anti-phospho-STAT6 (Tyr-641, 9361), rabbit anti-STAT6 (5397), rabbit anti-cleaved PARP (Asp-241, 9541), rabbit anti-caspase-3 (9662), rabbit anti-cleaved caspase-3 (Asp-175, 9661), or rabbit anti-GAPDH (2118) from Cell Signaling Technology.

RNA isolation

RNA was isolated at the indicated time points from T84 cells cultures on Transwell filters or frozen murine tissues using RNeasy mini kits (Qiagen).

Human colitis real-time tissue array

The human cDNA TissueScan Crohn's and Colitis Tissue qPCR Panel II (CCRT302; Origene) contained cDNA from 4 normal human colonic tissues, and colonic tissues from 21 UC and 5 CD patients. qPCR was performed as described below. Data were initially normalized to β-actin expression for cDNA content, and then normalized to the epithelial maker EpCAM (epithelial cell adhesion molecule) to control for epithelial cell content, because matriptase and prostasin are almost exclusively expressed in the intestinal epithelial cells (45, 66).

Quantitative PCR analysis

Reverse transcription and qPCR were performed using TaqMan Reverse Transcription and PCR Reagents (Life Technologies). The predesigned TaqMan primers used were human *ST14* (Hs00222707_m1); murine *St14* (Mm00487858_m1), human *PRSS8* (prostasin, Hs00173606_m1); murine *Prss8* (Prostasin, Mm00504792_m1), and murine *Epcam* (Mm00493214_m1). Data were normalized to human *GAPDH* (Hs99999905_m1), murine *Gapdh* (Mm99999915_g1), or human 18S rRNA (Hs99999901_s1) as indicated. Relative gene expression was calculated using the $2^{-\Delta\Delta CT}$ method (67).

Statistical analysis

Data are expressed as means ± S.E. or S.D., as indicated, and are representative of at least two independent experiments. Statistical analyses were performed using the two-tailed unpaired *t* test, or the two-tailed Mann-Whitney *U* test, as indicated. A threshold of $p < 0.05$ was considered significant.

Author contributions—M. S. B. designed and conducted most of the experiments, analyzed the results, and wrote the paper. T. A. J. and G. D. C. performed T84 barrier formation and disruption experiments, qPCR, and Western blotting. E. W. M. performed qPCR and Western blotting. S. M. analyzed human colitis arrays. T. S. D. helped design DSS-colitis experiments, isolated murine colitis tissues, and discussed results. T. M. A. designed the study, analyzed results, and wrote the paper. All authors reviewed and approved the final version of the manuscript.

Acknowledgments—We thank Thomas Bugge (NIH) for providing the St14 hypomorphic mouse strain, and Abatar Paudel for excellent technical laboratory assistance.

References

1. Xavier, R. J., and Podolsky, D. K. (2007) Unravelling the pathogenesis of inflammatory bowel disease. *Nature* **448,** 427–434
2. Michielan, A., and D'Incà, R. (2015) Intestinal permeability in inflammatory bowel disease: Pathogenesis, clinical evaluation, and therapy of leaky gut. *Mediators Inflamm.* **2015,** 628157
3. Hollander, D., Vadheim, C. M., Brettholz, E., Petersen, G. M., Delahunty, T., and Rotter, J. I. (1986) Increased intestinal permeability in patients with Crohn's disease and their relatives. A possible etiologic factor. *Ann. Intern. Med.* **105,** 883–885
4. Katz, K. D., Hollander, D., Vadheim, C. M., McElree, C., Delahunty, T., Dadufalza, V. D., Krugliak, P., and Rotter, J. I. (1989) Intestinal permeability in patients with Crohn's disease and their healthy relatives. *Gastroenterology* **97,** 927–931
5. Irvine, E. J., and Marshall, J. K. (2000) Increased intestinal permeability precedes the onset of Crohn's disease in a subject with familial risk. *Gastroenterology* **119,** 1740–1744
6. Jenkins, R. T., Ramage, J. K., Jones, D. B., Collins, S. M., Goodacre, R. L., and Hunt, R. H. (1988) Small bowel and colonic permeability to 51Cr-EDTA in patients with active inflammatory bowel disease. *Clin. Invest. Med.* **11,** 151–155
7. Fuss, I. J., Heller, F., Boirivant, M., Leon, F., Yoshida, M., Fichtner-Feigl, S., Yang, Z., Exley, M., Kitani, A., Blumberg, R. S., Mannon, P., and Strober, W. (2004) Nonclassical CD1d-restricted NK T cells that produce IL-13 characterize an atypical Th2 response in ulcerative colitis. *J. Clin. Invest.* **113,** 1490–1497
8. Heller, F., Florian, P., Bojarski, C., Richter, J., Christ, M., Hillenbrand, B., Mankertz, J., Gitter, A. H., Bürgel, N., Fromm, M., Zeitz, M., Fuss, I., Strober, W., and Schulzke, J. D. (2005) Interleukin-13 is the key effector Th2 cytokine in ulcerative colitis that affects epithelial tight junctions, apoptosis, and cell restitution. *Gastroenterology* **129,** 550–564
9. Fuss, I. J., and Strober, W. (2008) The role of IL-13 and NK T cells in experimental and human ulcerative colitis. *Mucosal. Immunol.* **Suppl 1,** S31–S33
10. Chen, M. L., and Sundrud, M. S. (2016) Cytokine networks and T-cell subsets in inflammatory bowel diseases. *Inflamm. Bowel. Dis.* **22,** 1157–1167
11. Bruewer, M., Luegering, A., Kucharzik, T., Parkos, C. A., Madara, J. L., Hopkins, A. M., and Nusrat, A. (2003) Proinflammatory cytokines disrupt epithelial barrier function by apoptosis-independent mechanisms. *J. Immunol.* **171,** 6164–6172
12. Utech, M., Mennigen, R., and Bruewer, M. (2010) Endocytosis and recycling of tight junction proteins in inflammation. *J. Biomed. Biotechnol.* **2010,** 484987
13. Prasad, S., Mingrino, R., Kaukinen, K., Hayes, K. L., Powell, R. M., MacDonald, T. T., and Collins, J. E. (2005) Inflammatory processes have dif-

ferential effects on claudins 2, 3 and 4 in colonic epithelial cells. *Lab. Invest.* **85,** 1139–1162

14. Zeissig, S., Bürgel, N., Günzel, D., Richter, J., Mankertz, J., Wahnschaffe, U., Kroesen, A. J., Zeitz, M., Fromm, M., and Schulzke, J. D. (2007) Changes in expression and distribution of claudin 2, 5 and 8 lead to discontinuous tight junctions and barrier dysfunction in active Crohn's disease. *Gut* **56,** 61–72
15. Randall, K., Henderson, N., Reens, J., Eckersley, S., Nystrom, A. C., South, M. C., Balendran, C. A., Bottcher, G., Hughes, G., and Price, S. A. (2016) Claudin-2 expression levels in ulcerative colitis: Development and validation of an in-situ hybridisation assay for therapeutic studies. *PLoS One* **11,** e0162076
16. Inoue, S., Matsumoto, T., Iida, M., Mizuno, M., Kuroki, F., Hoshika, K., and Shimizu, M. (1999) Characterization of cytokine expression in the rectal mucosa of ulcerative colitis: Correlation with disease activity. *Am. J. Gastroenterol.* **94,** 2441–2446
17. Weber, C. R., Raleigh, D. R., Su, L., Shen, L., Sullivan, E. A., Wang, Y., and Turner, J. R. (2010) Epithelial myosin light chain kinase activation induces mucosal interleukin-13 expression to alter tight junction ion selectivity. *J. Biol. Chem.* **285,** 12037–12046
18. Heller, F., Fuss, I. J., Nieuwenhuis, E. E., Blumberg, R. S., and Strober, W. (2002) Oxazolone colitis, a Th2 colitis model resembling ulcerative colitis, is mediated by IL-13-producing NK-T cells. *Immunity* **17,** 629–638
19. Fuss, I. J., Neurath, M., Boirivant, M., Klein, J. S., de la Motte, C., Strong, S. A., Fiocchi, C., and Strober, W. (1996) Disparate CD4+ lamina propria (LP) lymphokine secretion profiles in inflammatory bowel disease. Crohn's disease LP cells manifest increased secretion of IFN-gamma, whereas ulcerative colitis LP cells manifest increased secretion of IL-5. *J. Immunol.* **157,** 1261–1270
20. Mann, E. R., Bernardo, D., Ng, S. C., Rigby, R. J., Al-Hassi, H. O., Landy, J., Peake, S. T., Spranger, H., English, N. R., Thomas, L. V., Stagg, A. J., Knight, S. C., and Hart, A. L. (2014) Human gut dendritic cells drive aberrant gut-specific t-cell responses in ulcerative colitis, characterized by increased IL-4 production and loss of IL-22 and IFNγ. *Inflamm. Bowel. Dis.* **20,** 2299–2307
21. Tilg, H., and Kaser, A. (2015) Failure of interleukin 13 blockade in ulcerative colitis. *Gut* **64,** 857–858
22. Stevceva, L., Pavli, P., Husband, A., Ramsay, A., and Doe, W. F. (2001) Dextran sulphate sodium-induced colitis is ameliorated in interleukin 4 deficient mice. *Genes Immun.* **2,** 309–316
23. Boirivant, M., Fuss, I. J., Chu, A., and Strober, W. (1998) Oxazolone colitis: A murine model of T helper cell type 2 colitis treatable with antibodies to interleukin 4. *J. Exp. Med.* **188,** 1929–1939
24. Kasaian, M. T., Page, K. M., Fish, S., Brennan, A., Cook, T. A., Moreira, K., Zhang, M., Jesson, M., Marquette, K., Agostinelli, R., Lee, J., Williams, C. M., Tchistiakova, L., and Thakker, P. (2014) Therapeutic activity of an interleukin-4/interleukin-13 dual antagonist on oxazolone-induced colitis in mice. *Immunology* **143,** 416–427
25. List, K., Bugge, T. H., and Szabo, R. (2006) Matriptase: Potent proteolysis on the cell surface. *Mol. Med.* **12,** 1–7
26. Kosa, P., Szabo, R., Molinolo, A. A., and Bugge, T. H. (2012) Suppression of tumorigenicity-14, encoding matriptase, is a critical suppressor of colitis and colitis-associated colon carcinogenesis. *Oncogene* **31,** 3679–3695
27. List, K., Haudenschild, C. C., Szabo, R., Chen, W., Wahl, S. M., Swaim, W., Engelholm, L. H., Behrendt, N., and Bugge, T. H. (2002) Matriptase/MT-SP1 is required for postnatal survival, epidermal barrier function, hair follicle development, and thymic homeostasis. *Oncogene* **21,** 3765–3779
28. List, K., Kosa, P., Szabo, R., Bey, A. L., Wang, C. B., Molinolo, A., and Bugge, T. H. (2009) Epithelial integrity is maintained by a matriptase-dependent proteolytic pathway. *Am. J. Pathol.* **175,** 1453–1463
29. Buzza, M. S., Netzel-Arnett, S., Shea-Donohue, T., Zhao, A., Lin, C. Y., List, K., Szabo, R., Fasano, A., Bugge, T. H., and Antalis, T. M. (2010) Membrane-anchored serine protease matriptase regulates epithelial barrier formation and permeability in the intestine. *Proc. Natl. Acad. Sci. U.S.A.* **107,** 4200–4205
30. Netzel-Arnett, S., Buzza, M. S., Shea-Donohue, T., Désilets, A., Leduc, R., Fasano, A., Bugge, T. H., and Antalis, T. M. (2011) Matriptase protects against experimental colitis and promotes intestinal barrier recovery. *Inflamm. Bowel Dis.* **18,** 1303–1314
31. Buzza, M. S., Martin, E. W., Driesbaugh, K. H., Désilets, A., Leduc, R., and Antalis, T. M. (2013) Prostasin is required for matriptase activation in intestinal epithelial cells to regulate closure of the paracellular pathway. *J. Biol. Chem.* **288,** 10328–10337
32. Friis, S., Madsen, D. H., and Bugge, T. H. (2016) Distinct developmental functions of prostasin (CAP1/PRSS8) zymogen and activated prostasin. *J. Biol. Chem.* **291,** 2577–2582
33. Lee, M. S., Tseng, I. C., Wang, Y., Kiyomiya, K., Johnson, M. D., Dickson, R. B., and Lin, C. Y. (2007) Autoactivation of matriptase *in vitro*: Requirement for biomembrane and LDL receptor domain. *Am. J. Physiol. Cell Physiol.* **293,** C95–C105
34. Wang, J. K., Teng, I. J., Lo, T. J., Moore, S., Yeo, Y. H., Teng, Y. C., Kaul, M., Chen, C. C., Zuo, A. H., Chou, F. P., Yang, X., Tseng, I. C., Johnson, M. D., and Lin, C. Y. (2014) Matriptase autoactivation is tightly regulated by the cellular chemical environments. *PLoS. One.* **9,** e93899
35. Friis, S., Uzzun Sales, K., Godiksen, S., Peters, D. E., Lin, C. Y., Vogel, L. K., and Bugge, T. H. (2013) A matriptase-prostasin reciprocal zymogen activation complex with unique features: Prostasin as a non-enzymatic co-factor for matriptase activation. *J. Biol. Chem.* **288,** 19028–19039
36. Szabo, R., Uzzun Sales, K., Kosa, P., Shylo, N. A., Godiksen, S., Hansen, K. K., Friis, S., Gutkind, J. S., Vogel, L. K., Hummler, E., Camerer, E., and Bugge, T. H. (2012) Reduced prostasin (CAP1/PRSS8) activity eliminates HAI-1 and HAI-2 deficiency-associated developmental defects by preventing matriptase activation. *PLoS Genet.* **8**, e1002937
37. Spacek, D. V., Perez, A. F., Ferranti, K. M., Wu, L. K., Moy, D. M., Magnan, D. R., and King, T. R. (2010) The mouse frizzy (*fr*) and rat 'hairless' (fr^{CR}) mutations are natural variants of protease serine S1 family member 8 (*Prss8*). *Exp. Dermatol.* **19,** 527–532
38. Keppner, A., Malsure, S., Nobile, A., Auberson, M., Bonny, O., and Hummler, E. (2016) Altered prostasin (CAP1/Prss8) expression favors inflammation and tissue remodeling in DSS-induced colitis. *Inflamm. Bowel Dis.* **22,** 2824–2839
39. Okayasu, I., Hatakeyama, S., Yamada, M., Ohkusa, T., Inagaki, Y., and Nakaya, R. (1990) A novel method in the induction of reliable experimental acute and chronic ulcerative colitis in mice. *Gastroenterology* **98,** 694–702
40. Friis, S., Sales, K. U., Schafer, J. M., Vogel, L. K., Kataoka, H., and Bugge, T. H. (2014) The protease inhibitor HAI-2, but not HAI-1, regulates matriptase activation and shedding through prostasin. *J. Biol. Chem.* **289,** 22319–22332
41. Friis, S., Godiksen, S., Bornholdt, J., Selzer-Plon, J., Rasmussen, H. B., Bugge, T. H., Lin, C. Y., and Vogel, L. K. (2011) Transport via the transcytotic pathway makes prostasin available as a substrate for matriptase. *J. Biol. Chem.* **286,** 5793–5802
42. Selzer-Plon, J., Bornholdt, J., Friis, S., Bisgaard, H. C., Lothe, I. M., Tveit, K. M., Kure, E. H., Vogel, U., and Vogel, L. K. (2009) Expression of prostasin and its inhibitors during colorectal cancer carcinogenesis. *BMC Cancer* **9,** 201
43. Verghese, G. M., Gutknecht, M. F., and Caughey, G. H. (2006) Prostasin regulates epithelial monolayer function: Cell-specific Gpld1-mediated secretion and functional role for GPI anchor. *Am. J. Physiol. Cell Physiol* **291,** C1258-C1270
44. List, K., Szabo, R., Molinolo, A., Nielsen, B. S., and Bugge, T. H. (2006) Delineation of matriptase protein expression by enzymatic gene trapping suggests diverging roles in barrier function, hair formation, and squamous cell carcinogenesis. *Am. J. Pathol.* **168,** 1513–1525
45. List, K., Hobson, J. P., Molinolo, A., and Bugge, T. H. (2007) Co-localization of the channel activating protease prostasin/(CAP1/PRSS8) with its candidate activator, matriptase. *J. Cell. Physiol.* **213,** 237–245
46. Hebenstreit, D., Wirnsberger, G., Horejs-Hoeck, J., and Duschl, A. (2006) Signaling mechanisms, interaction partners, and target genes of STAT6. *Cytokine Growth Factor Rev.* **17,** 173–188
47. Rosen, M. J., Frey, M. R., Washington, M. K., Chaturvedi, R., Kuhnhein, L. A., Matta, P., Revetta, F. L., Wilson, K. T., and Polk, D. B. (2011) STAT6 activation in ulcerative colitis: A new target for prevention of IL-13-in-

duced colon epithelial cell dysfunction. *Inflamm. Bowel. Dis.* **17,** 2224–2234
48. Leyvraz, C., Charles, R. P., Rubera, I., Guitard, M., Rotman, S., Breiden, B., Sandhoff, K., and Hummler, E. (2005) The epidermal barrier function is dependent on the serine protease CAP1/Prss8. *J. Cell Biol.* **170,** 487–496
49. Ramsay, A. J., Dong, Y., Hunt, M. L., Linn, M., Samaratunga, H., Clements, J. A., and Hooper, J. D. (2008) Kallikrein-related peptidase 4 (KLK4) initiates intracellular signaling via protease-activated receptors (PARs). KLK4 and PAR-2 are co-expressed during prostate cancer progression. *J. Biol. Chem.* **283,** 12293–12304
50. Mildner, M., Bauer, R., Mlitz, V., Ballaun, C., and Tschachler, E. (2015) Matriptase-1 expression is lost in psoriatic skin lesions and is downregulated by TNFα *in vitro*. *J. Dtsch. Dermatol. Ges.* **13,** 1165–1174
51. Schroder, A. J., Pavlidis, P., Arimura, A., Capece, D., and Rothman, P. B. (2002) Cutting edge: STAT6 serves as a positive and negative regulator of gene expression in IL-4-stimulated B lymphocytes. *J. Immunol.* **168,** 996–1000
52. Hung, R.-J., Hsu, I.-W., Dreiling, J. L., Lee, M.-J., Williams, C. A., Oberst, M. D., Dickson, R. B., and Lin, C.-Y. (2004) Assembly of adherens junctions is required for sphingosine 1-phosphate-induced matriptase accumulation and activation at mammary epithelial cell-cell contacts. *Am. J. Physiol. Cell Physiol.* **286,** C1159–C1169
53. Ivanov, A. I., Nusrat, A., and Parkos, C. A. (2004) The epithelium in inflammatory bowel disease: Potential role of endocytosis of junctional proteins in barrier disruption. *Novartis Found. Symp.* **263,** 115–124
54. Ivanov, A. I., Nusrat, A., and Parkos, C. A. (2005) Endocytosis of the apical junctional complex: Mechanisms and possible roles in regulation of epithelial barriers. *Bioessays* **27,** 356–365
55. Rosen, M. J., Chaturvedi, R., Washington, M. K., Kuhnhein, L. A., Moore, P. D., Coggeshall, S. S., McDonough, E. M., Weitkamp, J. H., Singh, A. B., Coburn, L. A., Williams, C. S., Yan, F., Van Kaer, L., Peebles, R. S., Jr., and Wilson, K. T. (2013) STAT6 deficiency ameliorates severity of oxazolone colitis by decreasing expression of claudin-2 and Th2-inducing cytokines. *J. Immunol.* **190**:1849–1858
56. Glauben, R., Batra, A., Stroh, T., Erben, U., Fedke, I., Lehr, H. A., Leoni, F., Mascagni, P., Dinarello, C. A., Zeitz, M., and Siegmund, B. (2008) Histone deacetylases: Novel targets for prevention of colitis-associated cancer in mice. *Gut* **57,** 613–622
57. Glauben, R., Batra, A., Fedke, I., Zeitz, M., Lehr, H. A., Leoni, F., Mascagni, P., Fantuzzi, G., Dinarello, C. A., and Siegmund, B. (2006) Histone hyperacetylation is associated with amelioration of experimental colitis in mice. *J. Immunol.* **176,** 5015–5022
58. Amasheh, S., Meiri, N., Gitter, A. H., Schöneberg, T., Mankertz, J., Schulzke, J. D., and Fromm, M. (2002) Claudin-2 expression induces cation-selective channels in tight junctions of epithelial cells. *J. Cell Sci.* **115,** 4969–4976
59. Rosenthal, R., Milatz, S., Krug, S. M., Oelrich, B., Schulzke, J. D., Amasheh, S., Günzel, D., and Fromm, M. (2010) Claudin-2, a component of the tight junction, forms a paracellular water channel. *J. Cell Sci.* **123,** 1913–1921
60. Luettig, J., Rosenthal, R., Barmeyer, C., and Schulzke, J. D. (2015) Claudin-2 as a mediator of leaky gut barrier during intestinal inflammation. *Tissue Barriers* **3,** e977176
61. Behera, J., Jayprakash, V., and Sinha, B. N. (2015) Histone deacetylase inhibitors: A review on class-I specific inhibition. *Mini Rev. Med. Chem.* **15,** 731–750
62. Duvic, M., and Dimopoulos, M. (2016) The safety profile of vorinostat (suberoylanilide hydroxamic acid) in hematologic malignancies: A review of clinical studies. *Cancer Treat. Rev.* **43,** 58–66
63. Felice, C., Lewis, A., Armuzzi, A., Lindsay, J. O., and Silver, A. (2015) Review article: Selective histone deacetylase isoforms as potential therapeutic targets in inflammatory bowel diseases. *Aliment. Pharmacol. Ther.* **41,** 26–38
64. List, K., Currie, B., Scharschmidt, T. C., Szabo, R., Shireman, J., Molinolo, A., Cravatt, B. F., Segre, J., and Bugge, T. H. (2007) Autosomal ichthyosis with hypotrichosis syndrome displays low matriptase proteolytic activity and is phenocopied in ST14 hypomorphic mice. *J. Biol. Chem.* **282,** 36714–36723
65. Moolenbeek, C., and Ruitenberg, E. J. (1981) The "Swiss roll": A simple technique for histological studies of the rodent intestine. *Lab. Anim.* **15,** 57–59
66. Oberst, M. D., Singh, B., Ozdemirli, M., Dickson, R. B., Johnson, M. D., and Lin, C. Y. (2003) Characterization of matriptase expression in normal human tissues. *J. Histochem. Cytochem.* **51,** 1017–1025
67. Livak, K. J., and Schmittgen, T. D. (2001) Analysis of relative gene expression data using real-time quantitative PCR and the $2^{-\Delta\Delta CT}$ method. *Methods* **25,** 402–408